

Nucleophilic Attack toward Group 4 Metal Complexes Bearing Reactive 1-Aza-1,3-butadienyl and Imido Moieties

Hirofumi Hamaki, Nobuhiro Takeda, and Norihiro Tokitoh*

Institute for Chemical Research, Kyoto University, Gokasho, Uji, Kyoto 611-0011

Received November 1, 2006

Unique (1-aza-2-butenyl)titanium complexes bearing a phosphonium ylide moiety $[\text{Ti}=\text{NTbt}\{\text{C}(\text{Me})(\text{PR}_3)\text{CH}=\text{C}(\text{Me})\text{N}(\text{Mes})\}\text{Cl}]$ (**3–5**, Tbt = 2,4,6-tris[bis(trimethylsilyl)methyl]phenyl, Mes = 2,4,6-trimethylphenyl) were formed by the nucleophilic attack of PMe_3 , $\text{P}(n\text{-Bu})_3$, and 1,2-bis(dimethylphosphino)ethane (dmpe) toward the corresponding (1-aza-1,3-butadienyl)titanium complex, $[\text{Ti}=\text{NTbt}\{\text{C}(\text{Me})\text{CHC}(\text{Me})\text{N}(\text{Mes})\}\{\mu\text{-Cl}\}_2\text{Li}(\text{tmeda})]$ (**2a**). The reaction of a lithium β -diketiminato, $[\text{Li}\{\text{N}(\text{Tbt})\text{C}(\text{Me})\text{CHC}(\text{Me})\text{N}(\text{Mes})\}]$ (**1**) with $[\text{Ti}^{\text{IV}}\text{Cl}_2(\text{dmpe})_2]$ also resulted in the formation of the same complex **5**. Density functional theory calculation indicated that the negative charge of the model molecule of **3** was slightly delocalized to the C_3N plane. In addition, the calculation of the model molecule of **2a** suggested the electrophilicity of **2a** at the carbon atom connecting to the titanium atom. Interestingly, the reaction of zirconium and hafnium analogues (**2b** and **2c**) with PMe_3 and dmpe did not proceed. In contrast to the cases of phosphine reagents, pyridine which was found to undergo the nucleophilic attack toward the titanium center of **2a** gave the pyridine-coordinated titanium-imide $[\text{Ti}=\text{NTbt}\{\text{C}(\text{Me})\text{CHC}(\text{Me})\text{N}(\text{Mes})\}\text{Cl}(\text{py})]$ (**7**).

Introduction

Recently, much attention has been paid to the chemistry of β -diketiminato ligands bearing bulky substituents, such as a 2,6-diisopropylphenyl (Dip) group on the nitrogen atoms.¹ One of the interesting properties of these ligands is that they can stabilize low-valent transition metal and main-group metal complexes.² However, β -diketiminato complexes of low-valent early transition metals have been little investigated to date. In general, it is difficult to prepare divalent group 4 metal complexes because they are thermally unstable and immediately react with unsaturated substrates (e.g., $\text{C}\equiv\text{C}$,³ $\text{C}=\text{O}$,³ $\text{N}=\text{N}$,⁴ $\text{N}\equiv\text{N}$,^{5,7} etc.). Recently, Mindiola and co-

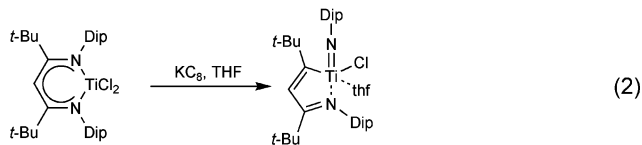
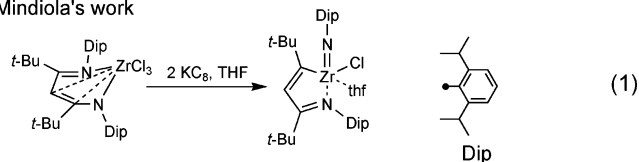
workers⁶ and Stephan and co-workers⁷ reported that the reductions of the β -diketiminato complexes of Zr(IV) and Ti(III) gave their respective ring-contracted imido complexes (Scheme 1, eqs 1–3). Furthermore, Stephan and co-workers reported that one-electron reduction of a $[\text{Ti}\{\text{[DipNC}(\text{Me})_2\text{CH}]\text{Cl}(\eta^5\text{-C}_5\text{H}_5)\}]$ under N_2 atmosphere resulted in the formation of a N_2 -activated β -diketiminato complex having putative Ti(II) centers (Scheme 1, eq 4).

On the other hand, we have reported the synthesis and structure of an unsymmetrical, extremely bulky lithium β -diketiminato, $[\text{Li}\{\text{N}(\text{Tbt})\text{C}(\text{Me})\text{CHC}(\text{Me})\text{N}(\text{Mes})\}]$ (**1**, Tbt = 2,4,6-tris[bis(trimethylsilyl)methyl]phenyl, Mes = 2,4,6-trimethylphenyl).⁸ In addition, independently of the studies reported by Mindiola and co-workers⁶ and Stephan and co-

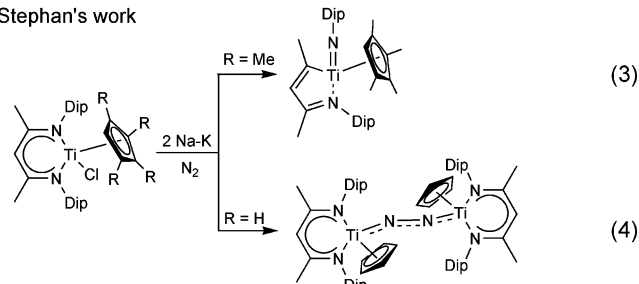
* To whom correspondence should be addressed. E-mail: tokitoh@boc.kuicr.kyoto-u.ac.jp.

- (1) Bourget-Merle, L.; Lappert, M. F.; Severn, J. R. *Chem. Rev.* **2002**, 102, 3031–3065.
- (2) (a) Smith, J. M.; Sadique, A. R.; Cundari, T. R.; Rodgers, K. R.; Lukat-Rodgers, G.; Lachicotte, R. J.; Flaschenriem, C. J.; Vela, J.; Holland, P. L. *J. Am. Chem. Soc.* **2006**, 128, 756–769. (b) Holland, P. L.; Cundari, T. R.; Perez, L. L.; Eckert, N. A.; Lachicotte, R. J. *J. Am. Chem. Soc.* **2002**, 124, 14416–14424. (c) Cheng, Y.; Hitchcock, P. B.; Lappert, M. F.; Zhou, M. *Chem. Commun.* **2005**, 752–754. (d) Driess, M.; Yao, S.; Brym, M.; van Wüllen, C.; Lentz, D. *J. Am. Chem. Soc.* **2006**, 128, 9628–9629.
- (3) (a) Eisch, J. J. *J. Organomet. Chem.* **2001**, 617–618, 148–157. (b) Eisch, J. J.; Shi, X.; Lasota, J. Z. *Naturforsch., B: Chem. Sci.* **1995**, 50, 342–350.
- (4) Duchateau, R.; Williams, A. J.; Gambarotta, S.; Chiang, M. Y. *Inorg. Chem.* **1991**, 30, 4863–4866.

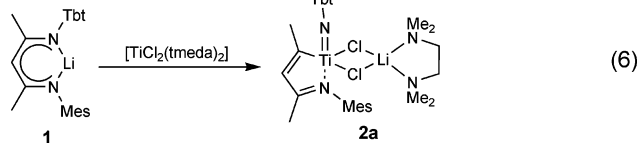
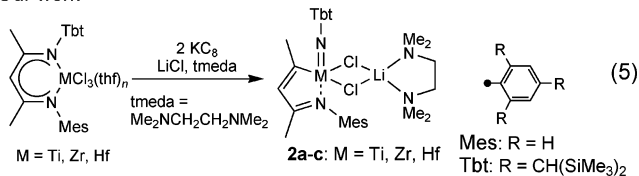
- (5) (a) MacLachlan, E. A.; Fryzuk, M. D. *Organometallics* **2006**, 23, 1530–1543. (b) Manriquez, J. M.; Sanner, R. D.; Marsh, R. E.; Bercaw, J. E. *J. Am. Chem. Soc.* **1976**, 98, 3042–3044. (c) Duchateau, R.; Gambarotta, S.; Beydoun, N.; Bensimon, C. *J. Am. Chem. Soc.* **1991**, 113, 8986–8988. (d) Hanna, T. E.; Keresztes, I.; Lobkovsky, E.; Bernskoetter, W. H.; Chirik, P. J. *Organometallics* **2004**, 23, 3448–3458.
- (6) (a) Basuli, F.; Kilgore, U. J.; Brown, D.; Huffman, J. C.; Mindiola, D. J. *Organometallics* **2004**, 23, 6166–6175. (b) Basuli, F.; Huffman, J. C.; Mindiola, D. J. *Inorg. Chim. Acta* **2007**, 360, 246–254.
- (7) Bai, G.; Wei, P.; Stephan, D. W. *Organometallics* **2006**, 25, 2649–2655.
- (8) (a) Takeda, N.; Hamaki, H.; Tokitoh, N. *Chem. Lett.* **2004**, 33, 134–135. (b) Hamaki, H.; Takeda, N.; Yamasaki, T.; Sasamori, T.; Tokitoh, N. *J. Organomet. Chem.* **2007**, 692, 44–54.

Scheme 1. Reductions of Group 4 Metal β -Diketiminates
Mindiola's work

Stephan's work

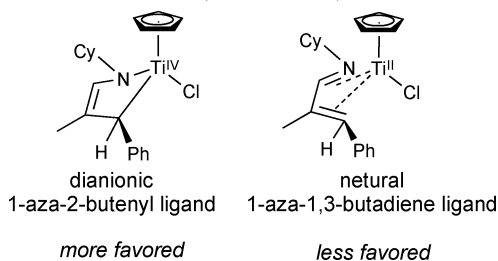
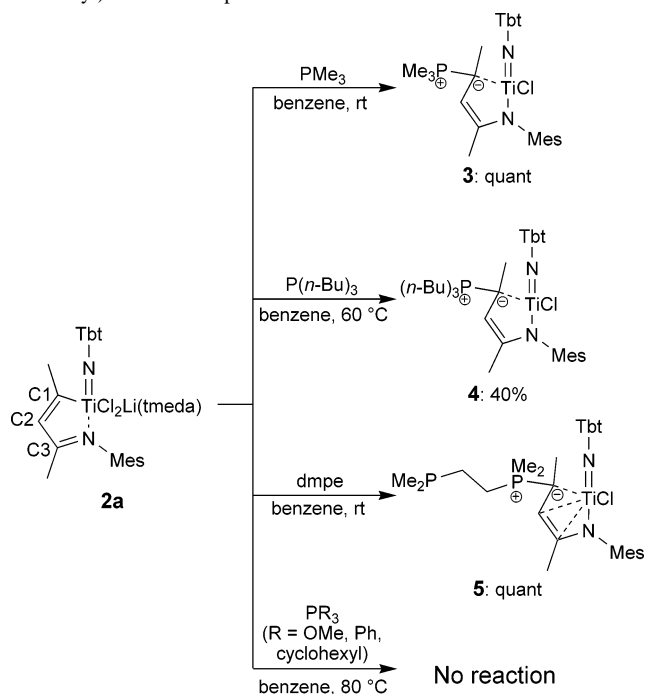


Our work



workers,⁷ we have found that the two-electron reduction of β -diketiminato complexes of Ti(IV), Zr(IV), and Hf(IV) derived from the lithium β -diketiminato **1** also gave imido complexes (**2a–c**) via a regioselective cleavage of the C–N bond of the intermediate M(II) complexes (Scheme 1, eq 5).⁹ The complexes **2a–c** have a monoanionic, planar 1-aza-1,3-butadienyl ligand. Furthermore, the possibility of a Ti(II) intermediate was supported by the reaction of lithium β -diketiminato (**1**) with [Ti^{II}Cl₂(tmeda)₂]¹⁰ (tmeda = Me₂NCH₂CH₂NMe₂), which resulted in the formation of the same complex **2a** (Scheme 1, eq 6).⁹

Although the group 4 metal complexes bearing a monoanionic, planar 1-aza-1,3-butadienyl moiety are rather rare species, some (1,3-butadienyl)metal complexes have been shown to be important intermediates in the catalytic cyclo-trimerization of alkynes and other catalytic transformations as well as a number of stoichiometric organometallic reactions.¹¹ The (heterobutadienyl)metal complexes such as monoazabutadienyl and diazabutadienyl complexes of group 4 metals can possibly activate the imine carbon atom toward

Scheme 2. Dianionic 1-Aza-2-butenyl and Neutral 1-Aza-1,3-butadiene Structure (Scholz's Work)**Scheme 3.** Nucleophilic Attack of Phosphines toward (1-Aza-1,3-butadienyl)titanium Complex

C–C coupling reactions (e.g., the 1,3-dipolar cycloaddition,^{12a} the ring expansion by use of electrophiles,^{12b} etc.). Specifically, Scholz and co-workers reported the titanium complex bearing a dianionic, nonplanar 1-aza-2-butenyl structure which is a more dominant electronic structure than the corresponding neutral 1-aza-1,3-butadiene structure (Scheme 2).¹³

In addition, the MeLi-induced α -proton elimination of (1-aza-2-butenyl)titanium complexes resulted in the formation of the corresponding titanium-carbene-ate complexes.¹⁴ However, the reactivity of (1-aza-1,3-butadienyl)metal complexes (**2a–c**), which have a conjugation pattern different from that of the Scholz complex, has not been disclosed yet.

In this report, we describe the nucleophilic attack of some nucleophiles such as phosphines, pyridine, and a sulfide

(9) Hamaki, H.; Takeda, N.; Tokitoh, N. *Organometallics* **2006**, *25*, 2457–2464.

(10) Edema, J. J. H.; Duchateau, R.; Gambarotta, S.; Hynes, R.; Gabe, E. *Inorg. Chem.* **1991**, *30*, 154–156.

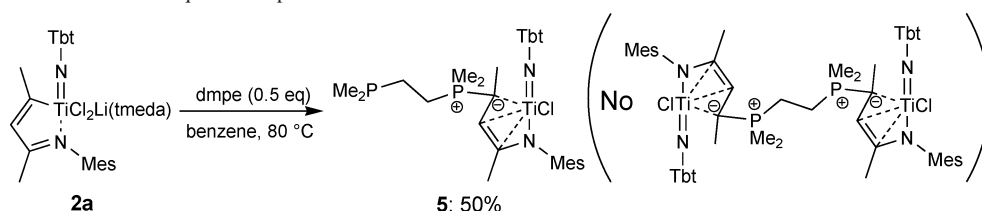
(11) (a) Yasuda, H.; Tatsumi, K.; Nakamura, A. *Acc. Chem. Res.* **1985**, *18*, 120–126. (b) Shore, N. E. *Chem. Rev.* **1988**, *88*, 1081–1119.

(12) (a) Scholz, J.; Görls, H. *Inorg. Chem.* **1996**, *35*, 4378–4382. (b) Scholz, J.; Kahlert, S.; Görls, H. *Organometallics* **1998**, *17*, 2876–2884.

(13) Scholz, J.; Kahlert, S.; Görls, H. *Organometallics* **2004**, *23*, 1594–1603.

(14) Kahlert, S.; Görls, H.; Scholz, J. *Angew. Chem., Int. Ed.* **1998**, *37*, 1857–1861.

(15) (a) Vincent, A. T.; Wheatley, P. J. *J. Chem. Soc., Dalton Trans.* **1972**, 617. (b) Amman, H.; Wheeler, G. L.; Watts, P. H., Jr. *J. Am. Chem. Soc.* **1973**, *95*, 6158–6163. (c) Erker, G.; Czlsch, P.; Krüger, C.; Wallis, J. M. *Organometallics* **1985**, *4*, 2059–2060.

Scheme 4. Reaction of **2a** with 0.5 equiv of dmpe

toward the titanium, zirconium, and hafnium imides (**2a–c**) bearing a 1-aza-1,3-butadienyl ligand. In these reactions, the selective nucleophilic attack was found to take place depending on the soft–hard character of the nucleophiles, although **2a–c** have many active sites such as the metal center, metal–imido bond, metal–carbon bond, and metal–nitrogen (of imine) bond.

Results and Discussion

Nucleophilic Attack of Phosphorus Compounds toward Titanium, Zirconium, and Hafnium Complexes (2a–c**) Bearing a 1-Aza-1,3-butadienyl Ligand.** The reaction of (1-aza-1,3-butadienyl)titanium (**2a**) with PMe_3 , $\text{P}(n\text{-Bu})_3$, and dmpe (dmpe = 1,2-bis(dimethylphosphino)ethane) resulted in the formation of the corresponding (1-aza-2-butenyl)-titanium complexes (**3–5**) bearing a phosphonium ylide moiety, while the reaction of **2a** with $\text{P}(\text{OMe})_3$, PPh_3 , and PCy_3 (Cy = cyclohexyl) did not occur (Scheme 3). No reactions of **2a** with $\text{P}(\text{OMe})_3$, PPh_3 , nor PCy_3 may be interpreted in terms of their weak nucleophilicity and steric hindrance. The reaction of **2a** with 0.5 equiv of dmpe gave no 2:1 adduct of **2a** with dmpe but yielded a 1:1 mixture of **5** and **2a** (Scheme 4). Moreover, the reaction of **2a** with an excess of dmpe afforded the same complex **5** together with free dmpe.

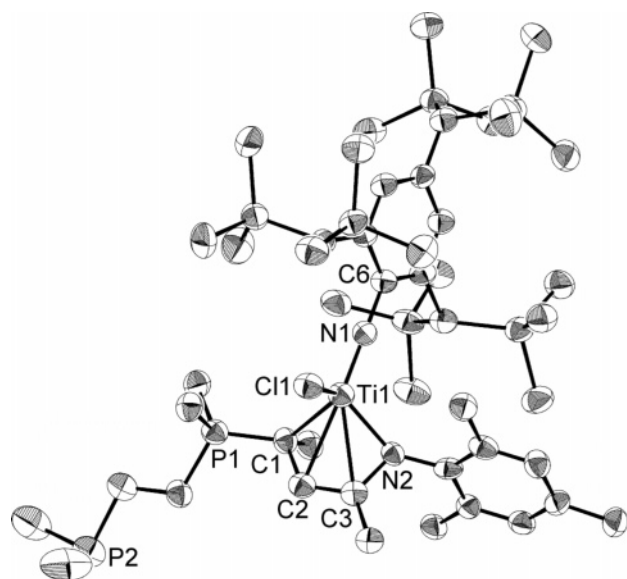
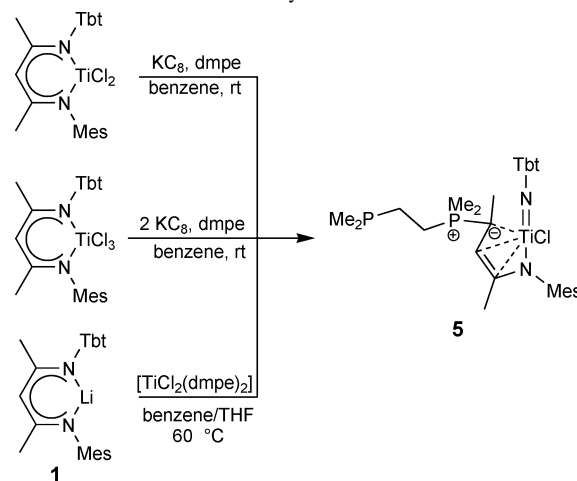
The (1-aza-2-butenyl)titanium complexes (**3–5**) were characterized by the ^1H , ^{13}C , and ^{31}P NMR spectra and elemental analysis. The ^1H and ^{13}C NMR spectra of **3** showed that the chemical shifts of the $\text{P}^+-\text{C1}^--\text{C2H}-\text{C3}$ part were

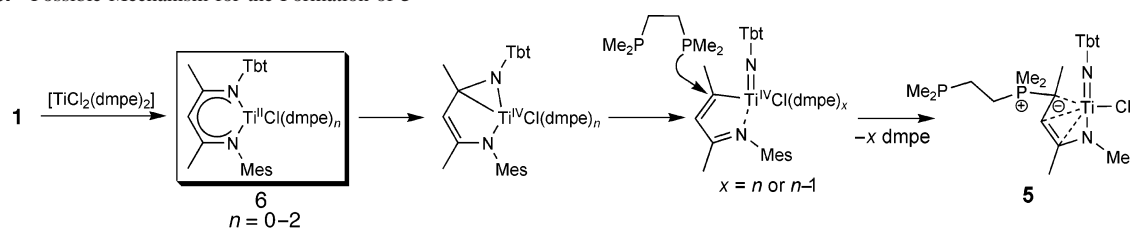
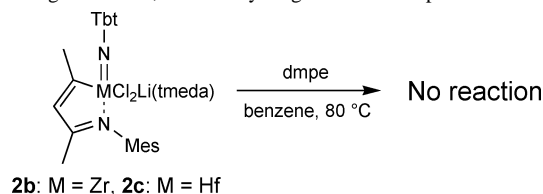
Table 1. Selected Bond Lengths (Å) and Angles (deg)

	5	2a^a	7
Ti–N1	1.721(5)	1.717(4)	1.732(4), 1.733(4)
Ti–C1	2.209(5)	2.192(5)	2.147(5), 2.165(5)
Ti···C2	2.464(6)	2.981(5)	2.968(5), 2.967(5)
Ti···C3	2.450(6)	2.994(5)	2.983(5), 2.997(5)
C1–C2	1.501(8)	1.339(7)	1.339(7), 1.338(7)
C2–C3	1.355(8)	1.448(7)	1.448(7), 1.451(7)
C3–N2	1.392(7)	1.296(6)	1.315(6), 1.301(6)
Ti–N2	1.952(5)	2.202(4)	2.199(4), 2.223(4)
Ti–N3			2.279(4), 2.251(4)
Ti–Cl1,	2.346(2)	2.4185(17),	2.3348(16),
Cl2		2.4223(17)	2.3262(16)
Ti–N1–C6	173.9(4)	175.1(3)	166.1(3), 167.3(3)
C1–Ti–N2	86.9(2)	75.50(16)	76.12(17), 75.96(17)

^a Reference 9.

observed in an upfield region [$\delta_{\text{H}} = 4.16$ (d, $^3J_{\text{PH}} = 19.4$ Hz), $\delta_{\text{C1}} = 45.3$ (d, $^1J_{\text{PC}} = 61.5$ Hz), $\delta_{\text{C2}} = 94.6$, $\delta_{\text{C3}} = 157.9$] compared with the chemical shifts of the C1–C2H–C3 part of **2a** [$\delta_{\text{H}} = 6.59$ (q, $^4J_{\text{PH}} = 1.4$ Hz), $\delta_{\text{C1}} = 237.2$, $\delta_{\text{C2}} = 132.6$, $\delta_{\text{C3}} = 180.8$]. Specifically, the ^{13}C NMR chemical shift of C1 for **3** appeared at a much higher field than that of **2a**. The $^{31}\text{P}\{^1\text{H}\}$ NMR spectrum of **3** was observed in 18.8 ppm. The reaction of **2a** with $\text{P}(n\text{-Bu})_3$ also resulted in the formation of the phosphonium-ylide analogue **4** in 40% yield [the characteristic chemical shifts in NMR spectra of the $\text{P}^+-\text{C1}^--\text{C2H}-\text{C3}$ part { $\delta_{\text{H}} = 4.54$ (d, $^3J_{\text{PH}} = 16.7$ Hz), $\delta_{\text{P}} = 27.1$ }], although the isolation of the ylide **4** was unsuccessful. The ^1H and ^{13}C NMR spectra of **5** showed the chemical shifts and the coupling constants of the $\text{P}^+-\text{C1}^--\text{C2H}-\text{C3}$ part [$\delta_{\text{H}} = 4.28$ (d, $^3J_{\text{PH}} = 18.2$ Hz), $\delta_{\text{C1}} = 45.6$ (d, $^1J_{\text{PC}} = 58.1$ Hz), $\delta_{\text{C2}} = 94.6$] as well as those of **3** and **4**. The $^{31}\text{P}\{^1\text{H}\}$ NMR spectrum of **5** exhibited two signals [$\delta_{\text{P}} = -45.1$ (d, $^3J_{\text{PP}} = 27$ Hz) and 24.2 (d, $^3J_{\text{PP}} = 27$ Hz)]. The NMR studies suggest that the C_3NTi rings of

**Figure 1.** ORTEP drawing of **5** (50% probability). The hydrogen atoms and solvent molecules are omitted for clarity.**Scheme 5.** Other Route of the Synthesis of **5**

Scheme 6. Possible Mechanism for the Formation of **5****Scheme 7.** Reaction of Zirconium and Hafnium Complexes (**2b** and **2c**) Bearing a 1-Aza-1,3-butadienyl Ligand with Phosphines

3–5 are more negative than that of **2a**, and the negative charges of **3–5** are mainly located on the C1 atom. In UV–vis spectra, the $\pi-\pi^*$ transitions of the C_3N ligand of **3** and **5** [λ_{\max} = 350 (ϵ = 11 000); **5**, 349 nm (ϵ = 11 000)] were red shifted compared with that of **2a** [318 nm (ϵ = 12 000)], which indicated some conjugation of the C_3N ligand.

The molecular structure of **5** was determined by X-ray crystallographic analysis. The ORTEP drawing of **5** is shown in Figure 1, and the selected bond lengths and angles are summarized in Table 1.

One can find many differences between the structure of **5** and that of **2a** as follows. First, the C_3N ligand of **5** can be considered to have the η^4 -coordination mode in contrast to the η^2 -coordination mode for **2a**. The Ti–C(ligand backbone) distances of **5** [2.464(6) (Ti–C2) and 2.450(6) Å (Ti–C3)] are still longer than those reported for the single Ti–C bond (Ti–C: 1.97–2.21 Å)¹⁷ but much shorter than those of **2a** [2.981(5) (Ti–C2) and 2.994(5) Å (Ti–C3)]. The central titanium atom of **5** deviates from the C_3N plane by 1.3125(67) Å, although the five-membered C_3NTi ring of **2a** is almost planar. Second, they differ from each other in the bond alternating pattern of the C_3NTi rings. In the case of **5**, the lengths of C1–C2 and C3–N2 bonds are both close to those of the corresponding single bonds, while those of **2a** are within the range of the corresponding double bond lengths.¹⁶ The C2–C3 bond lengths observed for **5** and **2a** are close to those of the C–C double and single bonds, respectively. That is, the C_3NTi rings of **5** and **2a** can be depicted mainly by the 1-titana-2-azacyclopenta-3-ene structure for **5** and 1-titana-2-azacyclopenta-2,4-diene one for **2a**. Although the bond alternating pattern of the C_3N ligand of **5** is similar to that of Scholz et al.'s titanium complex (Scheme 2),^{12b} it is different from that of Müller et al.'s 1-aza-

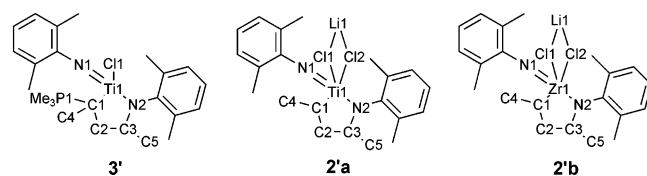
Table 2. Bond Lengths (Å) and Angles (deg) of the Optimized Structures of **3'**, **2'a**, and **2'b**^a

	3'	5 (obs.)	2'a	2a (obs.)	2'b	2b (obs.)
M–N1	1.710	1.721(5)	1.689	1.717(4)	1.852	1.8534(16)
M–C1	2.203	2.209(5)	2.174	2.192(5)	2.315	2.322(2)
C1–C2	1.502	1.501(8)	1.357	1.339(7)	1.360	1.347(3)
C2–C3	1.378	1.355(8)	1.453	1.448(7)	1.454	1.455(3)
C3–N2	1.394	1.392(7)	1.309	1.296(6)	1.312	1.301(3)
M–N2	1.977	1.952(5)	2.224	2.202(4)	2.335	2.3233(17)
M–Cl1	2.350	2.346(2)	2.539	2.4185(17)	2.697	2.5429(8)
M–Cl2			2.510	2.4223(17)	2.739	2.5481(8)
Li1–Cl1			2.195	2.285(8)	2.245	2.356(4)
Li1–Cl2			2.195	2.348(8)	2.247	2.362(4)
M–N1–C6	177.9	173.9(4)	175.075	175.1(3)	175.3	172.44(13)
C1–M–N2	87.6	86.9(2)	77.269	75.50(16)	73.7	72.53(7)

^a Calculated at the RB3LYP/6-31G(d) level and the observed structures of **5**, **2a**, and **2b**.

1,3-butadienyl complexes of late transition metals having almost equal C1–C2 and C2–C3 bond lengths.¹⁸ The Ti–N2 bond length of **5** is remarkably shorter than that of **2a**. The lengths of the Ti–C1 [2.209(5) Å] and Ti–N2 [1.952(5) Å] bonds for **5** are both within the range of the typical single bond values (Ti–C, 1.97–2.21, and Ti–N, 1.93–1.95 Å).¹⁷ The geometries around the C1 atom are pyramidal for **5** as evidenced by the summation of the bond angles around the C1 atom [338.3(5)°] in contrast to the trigonal planar geometry of **2a**. The C1–P1 bond length of **5** [1.751(6) Å] is longer than the typical phosphonium-ylide bond length (1.63–1.72 Å),¹⁵ although it is slightly shorter than the typical C–P single bond length (1.84–1.87 Å).¹⁶ In the case of **5**, there is no intermolecular contact between the P2 atom and the neighboring molecules ($P2\cdots Ti^* = 3.52$ Å).

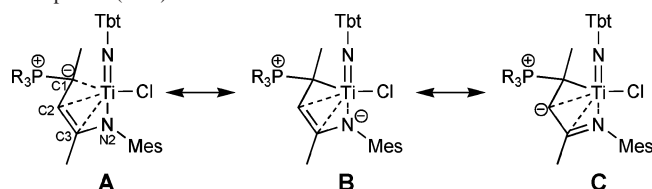
Since a carbon atom connecting to a Ti(IV) atom with a single bond is generally nucleophilic, it is very interesting that the C1 atom in the C_3NTi ring of **2a** has electrophilicity. An analogous nucleophilic attack of a phosphine to a carbon atom connecting to a Ti(IV) atom bearing a dianionic 1,3-butadienyl moiety has been reported by Rothwell and co-workers.¹⁹ However, this reaction involves the migration of a dimethylphenylsilyl substituent in one α -carbon to the other α -carbon, and hence it differs from our system. Girolami and co-workers reported that the reaction of $[Ti^{II}Me_2(dmpe)_2]$ with *trans,trans*-1,4-diphenyl-1,3-butadiene results in the displacement of one dmpe ligand and the generation of $[Ti^{II}$ -

Chart 1

- (16) Allen, F. H.; Kennard, O.; Watson, D. G.; Brammer, L.; Orpen, A. G.; Taylor, R. *J. Chem. Soc., Perkin Trans.* **1987**, S1–S19.
 (17) Orpen, A. G.; Brammer, L.; Allen, F. H.; Kennard, O.; Watson, D. G.; Taylor, R. *J. Chem. Soc., Perkin Trans.* **1989**, S1–S83.
 (18) tom Dieck, H.; Stamp, L.; Diercks, R.; Müller, C. *Nouv. J. Chim.* **1985**, 9, 289.
 (19) Balaich, G. J.; Fanwick, P. E.; Rothwell, I. P. *Organometallics* **1994**, 13, 4117–4118.

Table 3. Mulliken Atomic Charges of **3'**, **2'a**, and **2'b**

atomic number	3' (M = Ti)	2'a (M = Ti)	2'b (M = Zr)
M	0.851	0.897	1.319
C1	-0.361	-0.088	-0.144
C2	-0.244	-0.193	-0.180
C3	0.330	0.422	0.387
N1	-0.741	-0.593	-0.628
N2	-0.645	-0.673	-0.657
Cl1	-0.469	-0.363	-0.626
Cl2		-0.378	-0.638
P1	0.745		
Li1		0.349	0.555

Scheme 8. Resonance Structure of (1-Aza-2-butenyl)titanium Complexes (**3–5**)

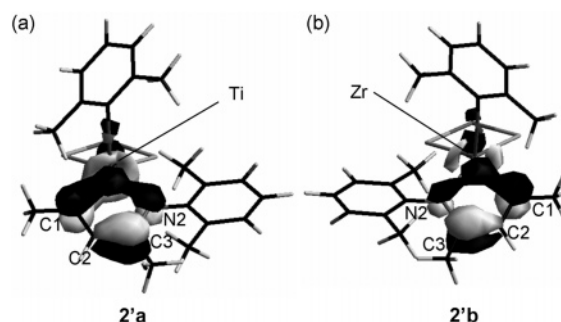
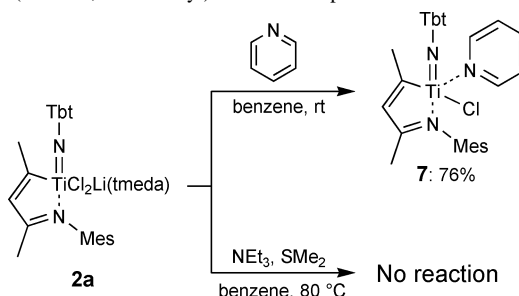
$\text{Me}_2(\eta^4\text{-}1,4\text{-C}_4\text{H}_4\text{Ph}_2)(\text{dmpe})$.²⁰ In this reaction, the nucleophilic attack of dmpe did not proceed toward the carbon atom connecting to the Ti(II) atom, although a free dmpe existed.

One- or two-electron reduction reactions of trivalent or tetravalent titanium β -diketiminates in the presence of dmpe were also found to result in the formation of the phosphonium ylide **5** (Scheme 5). In addition, the reaction of **1** with $[\text{TiCl}_2(\text{dmpe})_2]$ ²¹ allowed the same complex **5** in 60% yield (Scheme 5). Taking these results into consideration, the formation of **5** is most likely explained in terms of the initial generation of the corresponding divalent titanium complexes, $[\text{Ti}^{\text{II}}\text{Cl}\{\text{N}(\text{Tbt})\text{C}(\text{Me})\text{CHC}(\text{Me})\text{N}(\text{Mes})\}(\text{dmpe})_n]$ (**6**), followed by the ring contraction reaction and the subsequent nucleophilic attack of the P atom of dmpe to the C1 atom (Scheme 6).

By contrast to the case of the titanium complex (**2a**), no reactions were observed for the zirconium (**2b**) and hafnium analogues (**2c**) when they were treated with dmpe and PMe_3 in benzene at 80 °C (Scheme 7). The reasons for no nucleophilic attack toward the zirconium and hafnium complexes will be described later.

DFT Calculations of Mulliken Atomic Charges. The density functional theory (DFT) calculations of titanium imides **3'** and **2'a** and zirconium analogue **2'b**, where the Tbt, Mes, dmpe, and Li(tmeda) parts of **5**, **2a**, and **2b** were substituted by 2,6-dimethylphenyl (Dmp), Dmp, PMe_3 , and Li, respectively, were carried out at the RB3LYP level using the 6-31G(d) basis set, except using the LANL2DZ basis set on the Zr atom (Chart 1).

The optimized structures of the C_3NM rings of **3'**, **2'a**, and **2'b** are very similar to those of the C_3NM rings of **5**, **2a**, and **2b** experimentally obtained by X-ray structural analysis, indicating that the calculated results should be consistent with the properties of **5**, **2a**, and **2b** (Table 2).

**Figure 2.** LUMOs of **2'a** and **2'b**.**Scheme 9.** Nucleophilic Attack of Nitrogen and Sulfur Compounds toward (1-Aza-1,3-butadienyl)titanium Complex

The Mulliken atomic charges of **3'** and **2'a** (Table 3) showed important differences from each other. That is, the more negative charge population was located in the C_3NTi ring of **3'** rather than in that of **2'a** (the sum of the charges of the ring atoms: -0.165 for **3'**, 0.365 for **2'a**), and the negative charge population of **3'** was localized particularly on the C1 atom (-0.361 for **3'**, -0.088 for **2'a**).

These calculations on the charge population of **3'** indicated the large contribution of resonance structure **A**, where the negative charge is on the C1 atom, and a little contribution of structures **B** and **C**, where the negative charges are on the N2 and the C2 atoms, respectively (Scheme 8).

Scholz and co-workers reported the reaction of the (1-aza-2-butenyl)titanium complex with MeLi, and LiI afforded the titanium-carbene-ate complex $[\text{Ti}-\text{C}(\text{neighboring}): 1.958\text{--}(3) \text{ \AA}]$ with an emission of CH_4 .¹⁴ Rothwell and co-workers also reported that the reaction of the (cyclohexyl-condensed 1,3-butadiene)titanium complex with PMe_3 resulted in the formation of the short Ti–C bond [$1.956(7) \text{ \AA}$].¹⁹ However, the Ti–C1 bond of the (1-aza-2-butenyl)titanium complex **5** [$2.209(5) \text{ \AA}$] may not be classified as the above-mentioned titanium-carbene bond but as the intermediate between the single and the dative bonds shown in Scheme 8. Thus, the unique structure of the monoanionic, 1-aza-2-butenyl ligand of **5** was examined in detail by X-ray structural analysis and DFT calculations.

DFT Calculations of Molecular Orbitals. In the DFT calculations, the lowest unoccupied molecular orbital (LUMO) of **2'a** mainly consists of the d_{z^2} orbital of the Ti atom, which interacts with the p_x orbitals of the C1 and N2 atoms (Figure 2a). The nucleophilic attack of phosphines to the C1 atom in the reaction of **2a** is most likely interpreted in terms of the large contribution of the p_x orbital of the C1 atom to the LUMO. The nucleophilic attack to the N2 atom does not take place probably because of the negative charge and the

(20) Spencer, M. D.; Wilson, S. R.; Girolami, G. S. *Organometallics* **1997**, *16*, 3055–3067.

(21) (a) Girolami, G. S.; Wilkinson, G.; Galas, A. M. R.; Thornton-Pett, M.; Hursthouse, M. B. *J. Chem. Soc., Dalton Trans.* **1985**, 1339–1348. (b) Simpson, C. Q., II; Hall, M. B.; Guest, M. F. *J. Am. Chem. Soc.* **1991**, *113*, 2898–2903.

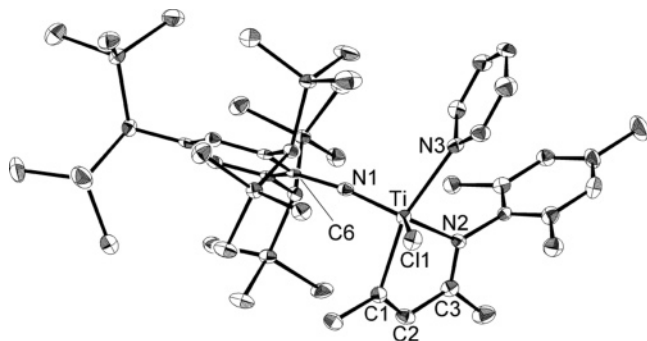


Figure 3. ORTEP drawing of **7** (50% probability). The hydrogen atoms and solvent molecules are omitted for clarity. One of the two independent molecules in the unit cell is depicted.

steric hindrance at the N2 atom, although the p orbital of the N2 atom has a similarly large contribution to the LUMO. In the case of zirconium, the p_x orbitals of the C1 and N2 atoms have a similarly large contribution to the LUMO (Figure 2b). However, the Mulliken atomic charge analysis showed important differences between **2'a** and **2'b**; that is, the more negative charge population was observed for the C1 atom of **2'b** (−0.144) than that of **2'a** (−0.088, Table 3). For this reason, the reactions of the zirconium and hafnium complexes (**2b** and **2c**) with dmpe and PMe_3 might not take place.

Nucleophilic Attack of Nitrogen and Sulfur Compounds toward (1-Aza-1,3-butadienyl)titanium Complex. The unique reactivity of the (1-aza-1,3-butadienyl)titanium complex **2a** prompted us to investigate the reactions of **2a** with nitrogen and sulfur compounds. Although the reactions of **2a** with NEt_3 and SMe_2 did not occur, the reaction of **2a** with pyridine resulted in the formation of the pyridine-coordinated titanium-imide **7** with the removal of $\text{LiCl}(\text{tmeda})$ (Scheme 9). That is, the nucleophilic attack of pyridine toward the titanium center rather than the C1 atom was due to the hard character of pyridine. The reaction of **1** with $[\text{Ti}^{\text{II}}\text{Cl}_2(\text{py})_4]^{22}$ also gave the same complex **7**.

Complex **7** was reasonably characterized by the ^1H and ^{13}C NMR spectra and elemental analysis, and its molecular structure was definitively determined by X-ray structural analysis (Figure 3 and Table 1). The ^{13}C NMR chemical shift of C1 for **7** is observed at a high field (237.1 ppm).

Two independent molecules are found in the unit cell of **7**, and both molecules have structures essentially similar to each other, except for the orientation of the pyridine ring to the TiC_3N plane [dihedral angles between the TiC_3N and pyridine planes are $87.9(4)$ and $68.4(4)^\circ$, respectively]. The Ti–N1 distances of **7** [1.732(4), 1.733(4) Å] are close to those of imido complexes **5** and **2a**. The C_3NTi ring of **7** is almost planar. Thus, the C_3NTi ring of **7** is consistent with that of 1-titana-2-azacyclopenta-2,4-diene as well as **2a**.

Conclusion

The (1-aza-2-butenyl)titanium complexes (**3**–**5**) bearing a phosphonium ylide moiety were formed by the nucleophilic

attack of PMe_3 , $\text{P}(n\text{-Bu})_3$, and dmpe toward the (1-aza-1,3-butadienyl)titanium complex **2a**. The reaction of the lithium β -diketiminate **1** with $[\text{TiCl}_2(\text{dmpe})_2]$ also resulted in the formation of the same complex **5**. The DFT calculation indicated that the negative charge in the ylide complex was mainly presented at the C1 atom and slightly delocalized to the C_3N plane. In addition, the calculation for the (1-aza-1,3-butadienyl)titanium system suggested the high electrophilicity at the C1 atom. On the other hand, the reactions of the zirconium and hafnium analogues **2b,c** with dmpe and PMe_3 did not proceed probably because of the more negative charge of the C1 atoms of the (1-aza-1,3-butadienyl)metal system, which were indicated by the Mulliken atomic charge calculations. Pyridine underwent the nucleophilic attack toward **2a** at the titanium center rather than the C1 atom, which reflected the hard character of pyridine. The investigations on the reactivities of **2a** toward other nucleophiles are currently in progress.

Experimental Section

General Considerations. Unless otherwise stated, all operations were performed in an MBRAUN Labmaster glovebox under an atmosphere of purified argon. Celite was activated at 200°C under vacuum for 1 day. $[\text{Li}\{\text{TbtNC}(\text{Me})\text{CHC}(\text{Me})\text{NMe}_2\}]$ (**1**),⁸ $[\text{TiCl}_2(\text{dmpe})_2]$,²¹ $[\text{TiCl}_2(\text{py})_4]$,²² $[\text{TiCl}_n\{\text{TbtNC}(\text{Me})\text{CHC}(\text{Me})\text{NMe}_2\}]$ ($n = 2, 3$),⁹ and $[\text{M}=\text{NTbt}\{\text{C}(\text{Me})\text{CHC}(\text{Me})\text{N}(\text{Mes})\}(\mu\text{-Cl})_2\text{Li}(\text{tmeda})]$ (**2a–c**)⁹ were prepared according to the methods described in the literature. ^1H NMR (300 MHz), ^{13}C NMR (75 MHz), and ^{31}P NMR (121 MHz) spectra were recorded on a JEOL JNM AL-300 spectrometer. The ^1H NMR chemical shifts were reported with reference to the internal residual $\text{C}_6\text{D}_5\text{H}$ (7.15 ppm). The ^{13}C NMR chemical shifts were reported with reference to the carbon-13 signal of C_6D_6 (128.0 ppm). Multiplicity of signals in ^{13}C NMR spectra was determined by DEPT techniques. The ^{31}P NMR chemical shifts were reported with reference to the external standards, 85% H_3PO_4 (0 ppm). Electronic spectra were recorded on a JASCO V-570 UV–vis spectrometer. Melting points were determined on a Yanaco micro melting point apparatus and are uncorrected. Elemental analyses were carried out at the Microanalytical Laboratory of the Institute for Chemical Research, Kyoto University.

Reaction of $[\text{Ti}=\text{NTbt}\{\text{C}(\text{Me})\text{CHC}(\text{Me})\text{N}(\text{Mes})\}(\mu\text{-Cl})_2\text{Li}(\text{tmeda})]$ (2a**) with PMe_3 .** PMe_3 (93 μL , 900 μmol) was added to a solution of **2a** (300.1 mg, 297.5 μmol) in benzene (8 mL). The reaction mixture was stirred for 3 h at room temperature, and the solvent was removed under reduced pressure. Benzene was added to the red residue, and the filtration through Celite gave a dark red solution. The filtrate was dried under vacuum, and the product was recrystallized from toluene at -40°C yielding the almost pure product as dark red crystals $[\text{Ti}=\text{NTbt}\{\text{C}(\text{Me})\text{CHC}(\text{Me})\text{N}(\text{Mes})\}\text{Cl}]$ (**3**, 272.7 mg, 99%). **3**: mp $213.4\text{--}216.3^\circ\text{C}$ (dec). ^1H NMR (300 MHz, C_6D_6 , 25°C): δ 0.24 (s, 36H), 0.43 (s, 18H), 0.79 (d, $^2J_{\text{PH}} = 12.7$ Hz, 9H), 1.43 (s, 1H), 1.54 (d, $^3J_{\text{PH}} = 20.3$ Hz, 3H), 1.85 (s, 3H), 2.20 (s, 3H), 2.40 (s, 3H), 2.84 (s, 3H), 3.58 (br s, 1H), 3.98 (br s, 1H), 4.16 (d, $^3J_{\text{PH}} = 18.2$ Hz, 1H), 6.47 (br s, 1H), 6.59 (br s, 1H), 6.87 (s, 1H), 6.90 (s, 1H). $^{13}\text{C}\{^1\text{H}\}$ NMR (75 MHz, C_6D_6 , 25°C): δ 1.07 (CH_3), 1.37 (CH_3), 10.0 (d, $^1J_{\text{PC}} = 57.2$ Hz, CH_3), 15.1 (CH_3), 20.0 (CH_3), 20.8 (CH_3), 21.0 (CH_3), 21.2 (CH), 22.2 (CH), 22.5 (CH_3), 29.8 (CH), 45.3 (d, $^1J_{\text{PC}} = 61.5$ Hz), 94.6 (CH), 121.6 (CH), 126.4 (CH), 129.6 (CH), 130.07 (CH), 130.13, 132.4, 132.5, 137.7, 138.1, 142.9, 143.2, 147.0, 157.9. $^{31}\text{P}\{^1\text{H}\}$ NMR (121 MHz, C_6D_6 , 25°C): δ 18.8 (s). UV–vis

(22) Araya, M. A.; Cotton, F. A.; Matonic, J. H.; Murillo, C. A. *Inorg. Chem.* **1995**, *34*, 5424–5428.

(*n*-hexane): λ_{\max} 280 (ϵ , 1.9×10^4), 350 (ϵ , 1.1×10^4), 469 (2.8×10^3) nm. Anal. Calcd for $C_{44}H_{86}N_2Si_6PClTi$: C, 57.07; H, 9.36; N, 3.03. Found: C, 57.34; H, 9.27; N, 3.31.

Reaction of 2a with P(*n*-Bu)₃. To a mixture of **2a** (99.9 mg, 99.2 μ mol) and P(*n*-Bu)₃ (75 μ L, 300 μ mol) in a NMR tube was added 0.6 mL of C₆D₆. After the NMR tube was sealed, degassed, and heated at 80 °C for 2 days, the measurement of the ¹H NMR spectrum revealed that the reaction proceeds to form [Ti{C(Me)-{P(*n*-Bu)₃}CH=C(Me)N(Mes)}Cl(NTbt)] **4** (ca. 40% in NMR yield). **4**: ¹H NMR (300 MHz, C₆D₆, 25 °C): δ 0.14 (s, 36H), 0.14 (s, 18H), 0.15 (s, 18H), 0.19 (s, 18H), 0.88 (m, 6H), 1.30–1.40 (m, 1 + 18H), 1.81 (s, 3H), 2.18 (s, 3H), 2.35 (s, 3H), 2.82 (s, 3H), 3.90 (br, 2H), 4.54 (d, ³J_{PH} = 16.7 Hz), 6.42–6.48 (br, 2H), 6.82 (s, 2H). ³¹P{¹H} NMR (121 MHz, C₆D₆, 25 °C): δ 27.1 (s).

Reaction of 2a with dmpe (1.0 equiv). dmpe (17 μ L, 100 μ mol) was added to a solution of **2a** (100.1 mg, 99.16 μ mol) in benzene (2 mL). The reaction mixture was stirred for 3 h at room temperature, and the solvent was removed under reduced pressure. Benzene was added to the red residue, and the filtration through Celite gave a dark red solution. The filtrate was evaporated under vacuum, and the residual product was recrystallized from toluene at –40 °C, yielding the almost pure product **5** (97.2 mg, 98%) as dark red crystals. **5**: mp 264.2–267.3 °C (dec). ¹H NMR (300 MHz, C₆D₆, 25 °C): δ 0.22 (s, 36H), 0.41 (s, 18H), 0.72 (d, ²J_{PH} = 4.0 Hz, 6H), 1.02 (d, ²J_{PH} = 12.5 Hz, 6H), 1.18–1.28 (m, 2H + 2H), 1.41 (s, 1H), 1.62 (d, ³J_{PH} = 19.6 Hz, 3H), 1.83 (s, 3H), 2.18 (s, 3H), 2.40 (s, 3H), 2.81 (s, 3H), 3.63 (br s, 1H), 3.99 (br s, 1H), 4.28 (d, ³J_{PH} = 18.2 Hz, 1H), 6.46 (br s, 1H), 6.57 (br s, 1H), 6.84 (s, 1H), 6.89 (s, 1H). ¹³C{¹H} NMR (75 MHz, C₆D₆, 25 °C): δ 1.4 (CH₃), 2.1 (CH₃), 8.5 (dd, ¹J_{PC} = 58.1 Hz, ⁴J_{PC} = 19.4 Hz, CH₃), 13.7 (dd, ¹J_{PC} = 15.1 Hz, ⁴J_{PC} = 5.6 Hz, CH₃), 15.7 (CH₃), 20.5 (CH₃), 20.8 (dd, ¹J_{PC} = 47.5 Hz, ²J_{PC} = 15.2 Hz, CH₂), 21.15 (CH₃), 21.4 (CH₃), 21.6 (CH), 22.8 (CH₃), 23.0 (CH), 24.1 (dd, ¹J_{PC} = 18.0 Hz, ²J_{PC} = 6.5 Hz, CH₂), 30.1 (CH), 45.6 (d, ¹J_{PC} = 58.1 Hz), 95.2 (CH), 121.6 (CH), 126.5 (CH), 129.6 (CH), 130.08 (CH), 130.14, 132.46, 132.49, 137.7, 138.1, 142.7, 143.0, 146.9, 157.9. ³¹P{¹H} NMR (121 MHz, C₆D₆, 25 °C): δ –45.1 (d, ³J_{PP} = 27 Hz), 24.2 (d, ³J_{PP} = 27 Hz). UV–vis (*n*-hexane): λ_{\max} 281 (ϵ , 1.9×10^4), 349 (1.1×10^4), 463 (2.8×10^3) nm. Anal. Calcd for $C_{47}H_{93}N_2Si_6PClTi$: C, 56.45; H, 9.37; N, 2.80. Found: C, 56.19; H, 9.53; N, 2.76.

Reactions of 2a with P(OMe)₃, PPh₃, and PCy₃. To mixtures of **2a** (100.1 mg, 99.3 μ mol) and P(OMe)₃ (35 μ L, 300 μ mol), **2a** (40.0 mg, 39.7 μ mol) and PPh₃ (31.2 mg, 159 μ mol), and **3a** (40.0 mg, 39.7 μ mol) and PCy₃ (13.3 mg, 159 μ mol) in NMR tubes was added 0.6 mL of C₆D₆. After the NMR tubes were sealed, degassed, and heated at 80 °C for 2 days, the measurement of the ¹H NMR spectra revealed that the reactions did not proceed.

Reaction of 2a with dmpe (0.5 equiv). To a mixture of **2a** (199.9 mg, 199.1 μ mol) and dmpe (17 μ L, 100 μ mol) in a NMR tube was added 0.6 mL of C₆D₆. The NMR tube was sealed, degassed, and heated at 80 °C for 2 days. The ¹H NMR spectrum showed the formation of a mixture of **5** and **2a** (50:50 **5/2a**).

Reaction of 2a with dmpe (5.0 equiv). To a mixture of **2a** (50.0 mg, 49.6 μ mol) and dmpe (42 μ L, 248 μ mol) in a NMR tube was added 0.6 mL of C₆D₆. The NMR tube was sealed and degassed. The ¹H and ³¹P NMR spectra showed the formation of **5** and a free dmpe.

Reaction of [Li{TbtNC(Me)CHC(Me)NMe₃}] (1**) with [TiCl₂(dmpe)₂].** To a mixture of **1** (40.1 mg, 51.7 μ mol) and [TiCl₂(dmpe)₂] (28.2 mg, 67.2 μ mol) in a NMR tube were added 0.3 mL of C₆D₆ and 0.3 mL of tetrahydrofuran (THF). After the NMR tube

was degassed and sealed, the measurement of the ¹H NMR spectrum revealed that the reaction did not proceed. After the sealed tube was heated at 60 °C for 2 days, the measurement of the ¹H NMR spectrum revealed the formation of a mixture of **5** and **1** (60:40 **5/1**).

One-Electron Reduction of [TiCl₂{TbtNC(Me)CHC(Me)NMe₃}] with KC₈. KC₈ (11.8 mg, 87.0 μ mol) was added to a solution of [TiCl₂{TbtNC(Me)CHC(Me)NMe₃}] (70.0 mg, 79.1 μ mol) in benzene (2 mL) and dmpe (17 μ L, 100 μ mol). The reaction mixture was stirred for 1 day at room temperature, and the solvent was removed under reduced pressure. Benzene was added to the red residue, and the filtration through Celite gave a dark red solution. The filtrate was evaporated under vacuum, and the residual product was recrystallized from toluene at –40 °C, yielding the almost pure product **5** (64.0 mg, 81%) as dark red crystals.

Two-Electron Reduction of [TiCl₃{TbtNC(Me)CHC(Me)NMe₃}] with KC₈. KC₈ (19.4 mg, 144 μ mol) was added to a solution of [TiCl₃{TbtNC(Me)CHC(Me)NMe₃}] (60.1 mg, 65.3 μ mol) in benzene (2 mL) and dmpe (17 μ L, 100 μ mol). The reaction mixture was stirred for 1 day at room temperature, and the solvent was removed under reduced pressure. Benzene was added to the red residue, and the filtration through Celite gave a dark red solution. The filtrate was evaporated under vacuum, and the residual product was recrystallized from toluene at –40 °C, yielding the almost pure product **5** (54.2 mg, 83%) as dark red crystals.

Reactions of [Zr=NTbt{C(Me)CHC(Me)N(Mes)}](μ -Cl)₂Li-(tmeda)] (2b**) and [Hf=NTbt{C(Me)CHC(Me)N(Mes)}](μ -Cl)₂Li-(tmeda)] (**2c**) with PMe₃ and dmpe.** To mixtures of **2b** (52.6 mg, 50.0 μ mol) and PMe₃ (16 μ L, 150 μ mol), **2b** (52.6 mg, 50.0 μ mol) and dmpe (9 μ L, 60 μ mol), **2c** (57.0 mg, 50.0 μ mol) and PMe₃ (16 μ L, 150 μ mol), and **2c** (57.0 mg, 50.0 μ mol) and dmpe (9 μ L, 60.0 μ mol) in NMR tubes was added 0.6 mL of C₆D₆. After the NMR tubes were degassed, sealed, and heated at 80 °C for 2 days, the measurement of the ¹H NMR spectra revealed the reactions did not proceed.

Reaction of 2a with Pyridine. Pyridine (40 μ L, 496 μ mol) was added to a solution of **2a** (100.2 mg, 99.2 μ mol) in benzene (2 mL). The reaction mixture was stirred for 3 h at room temperature, and the solvent was removed under reduced pressure. Benzene was added to the red residue, and the filtration through Celite gave a dark red solution. The filtrate was dried under vacuum, and the product was recrystallized from toluene at –40 °C, yielding the almost pure product as dark red crystals [Ti=NTbt{C(Me)CHC(Me)N(Mes)}Cl(py)] (**7**, 84.8 mg, 92%). **7**: mp 162–164 °C (dec). ¹H NMR (300 MHz, C₆D₆, 25 °C): δ 0.16 (s, 18H), 0.21 (s, 18H), 0.28 (s, 18H), 1.44 (s, 1H), 1.48 (s, 3H), 2.07 (s, 6H), 2.09 (s, 3H), 2.22 (d, ⁴J_{HH} = 1.3 Hz, 3H), 2.87 (br s, 1H), 2.93 (br s, 1H), 6.47 (br s, 1H), 6.51 (br s, 1H), 6.57 (q, ⁴J_{HH} = 1.3 Hz, 1H), 6.67 (m, 2H), 6.73 (m, 1H), 8.86 (m, 2H). ¹³C{¹H} NMR (75 MHz, C₆D₆): δ 1.1 (CH₃), 1.5 (CH₃), 2.0 (CH₃), 18.3 (CH₃), 20.8 (CH₃), 21.0 (CH₃), 21.3 (CH), 22.3 (CH₃), 29.4 (CH), 30.3 (CH), 124.1 (CH), 125.9 (CH), 128.9 (CH), 129.1 (CH), 130.5, 131.6 (CH), 132.5, 134.1, 134.9, 135.7 (CH), 136.6, 144.0, 151.1 (CH), 162.3, 199.0, 237.1. UV–vis (*n*-hexane): λ_{\max} 284 (ϵ , 1.9×10^4), 319 (ϵ , 1.2×10^4), 410 (1.8×10^3) nm. Anal. Calcd for $C_{46}H_{82}N_3Si_6ClTi$: C, 59.47; H, 8.90; N, 4.52. Found: C, 59.11; H, 8.96; N, 4.63.

Reactions of 3a with NEt₃ and SMe₂. To mixtures of **3a** (40.0 mg, 39.7 μ mol) and NEt₃ (199 μ L, 200 μ mol) and **3a** (99.8 mg, 99.2 μ mol) and SMe₂ (36 μ L, 500 μ mol) in NMR tubes was added 0.6 mL of C₆D₆. After the NMR tubes were degassed, sealed, and heated at 80 °C for 2 days, the measurement of the ¹H NMR spectra revealed the reactions did not proceed.

Reaction of 1 with [TiCl₂(py)₄]. A solution of **1** (40.0 mg, 51.7 μ mol) in benzene (2 mL) was added to [TiCl₂(py)₄] (29.2 mg, 67.4 μ mol). The reaction mixture was stirred for 1 day at room temperature, causing the change of dark blue color into dark red color, and the solvent was removed under reduced pressure. Benzene was added to the red residue, and the filtration through Celite gave a dark red solution. The filtrate was dried under vacuum, and the product was recrystallized from toluene at -40°C yielding the almost pure product as dark red crystals **7** (41.8 mg, 87%).

X-ray Crystallography. Single crystals of **5** and **7** were grown by the slow evaporation of the saturated toluene/hexane solution at -40°C . The preparation of this sample consisted of coating the crystal with silicon grease, mounting it on a glass fiber, and placing it under a cold stream of N₂ on the diffractometer. The intensity data of **5** and **7** were collected on a Rigaku/MSC mercury charged-coupled device (CCD) diffractometer with graphite monochromated Mo K α radiation ($\lambda = 0.71071\text{ \AA}$) to $2\theta_{\text{max}} = 50^{\circ}$ at 93 K. The structures of **5** and **7** were solved by direct method (SIR97).²³ All crystallographic data were refined by a full-matrix least-squares procedure on F^2 for all reflections (SHELXL-97).²⁴ All of the non-hydrogen atoms of **5** and **7** were placed using AFIX instruction. Crystal data for **5**: C₄₇H₉₃ClN₂P₂Si₆Ti \cdot C₇H₈, $M = 1092.20$, triclinic, space group $P\bar{1}$ (No. 2), $a = 11.8582(13)$, $b = 16.745(2)$, $c = 18.135(4)\text{ \AA}$, $\alpha = 98.209(17)^{\circ}$, $\beta = 101.840(15)^{\circ}$, $\gamma = 107.231(5)^{\circ}$, $V = 3285.4(10)\text{ \AA}^3$, $Z = 2$, $D_{\text{calcd}} = 1.104\text{ g cm}^{-3}$, $R_1(I > 2\sigma(I)) = 0.0818$, $wR2$ (all data) = 0.1938, $T = 103(2)\text{ K}$, GOF = 1.030, CCDC 615 249. Crystal data for **7**: C₄₆H₈₂ClN₃Si₆Ti \cdot 0.5C₆H₁₄, $M = 972.12$, triclinic, space group $P\bar{1}$ (No. 2), $a = 12.368(5)$, $b = 18.983(8)$, $c = 27.134(10)\text{ \AA}$, $\alpha = 106.011(4)^{\circ}$, $\beta = 90.942(2)^{\circ}$, $\gamma = 108.792(5)^{\circ}$, $V = 5758(4)\text{ \AA}^3$, $Z = 4$, $D_{\text{calcd}} = 1.121\text{ g cm}^{-3}$, $R_1(I$

$> 2\sigma(I)) = 0.0868$, $wR2$ (all data) = 0.2276, $T = 103(2)\text{ K}$, GOF = 1.112, CCDC 627 560.

Computational Methods. The geometries of [Ti{C(Me)(PMe₃)-CH=C(Me)N(Dmp)}Cl(NDmp)] (**3'**), [Ti=NDmp{C(Me)CHC(Me)N(Dmp)}(μ -Cl)₂Li] (**2'a**), and [Ti=NDmp{C(Me)CHC(Me)N(Dmp)}(μ -Cl)₂Li] (**2'b**) were optimized by using the Gaussian 98 program²⁵ at RB3LYP/6-31G(d), except the LANL2DZ basis set was used on the Zr atom.

Acknowledgment. This work was partially supported by Grants-in-Aid for Scientific Research [Nos. 12CE2005, 17GS0207, 14078213, and 15750031] and the 21 COE Program on Kyoto University Alliance for Chemistry from the Ministry of Education, Culture, Sports, Science and Technology, Japan. We are grateful to Dr. Takahiro Sasamori, Institute for Chemical Research, Kyoto University, for valuable discussions.

Supporting Information Available: Crystallographic information files for **5** and **7**, and Cartesian coordination and molecular orbitals of the optimized structures for **3'**, **2'a**, and **2'b**. This material is available free of charge via the Internet at <http://pubs.acs.org>.

IC0620844

- (23) Altomare, A.; Burla, M. C.; Camalli, M.; Cascarano, G. L.; Giacovazzo, C.; Guagliardi, A.; Moliterni, A. G. G.; Polidori, G.; Spagna, R. *J. Appl. Crystallogr.* **1999**, 32, 115–119.
 (24) Sheldrick, G. M. *SHELX-97, Program for the Refinement of Crystal Structures*; University of Göttingen: Göttingen, Germany, 1997.

- (25) Frisch, M. J.; Trucks, G. W.; Schlegel, H. B.; Scuseria, G. E.; Robb, M. A.; Cheeseman, J. R.; Zakrzewski, V. G.; Montgomery, J. A., Jr.; Stratmann, R. E.; Burant, J. C.; Dapprich, S.; Millam, J. M.; Daniels, A. D.; Kudin, K. N.; Strain, M. C.; Farkas, O.; Tomasi, J.; Barone, V.; Cossi, M.; Cammi, R.; Mennucci, B.; Pomelli, C.; Adamo, C.; Clifford, S.; Ochterski, J.; Petersson, G. A.; Ayala, P. Y.; Cui, Q.; Morokuma, K.; Malick, D. K.; Rabuck, A. D.; Raghavachari, K.; Foresman, J. B.; Cioslowski, J.; Ortiz, J. V.; Stefanov, B. B.; Liu, G.; Liashenko, A.; Piskorz, P.; Komaromi, I.; Gomperts, R.; Martin, R. L.; Fox, D. J.; Keith, T.; Al-Laham, M. A.; Peng, C. Y.; Nanayakkara, A.; Gonzalez, C.; Challacombe, M.; Gill, P. M. W.; Johnson, B. G.; Chen, W.; Wong, M. W.; Andres, J. L.; Head-Gordon, M.; Replogle, E. S.; Pople, J. A. *Gaussian 98*, revision A.6; Gaussian, Inc.: Pittsburgh, PA, 1998.